





# Exploring the universal $\bar{I} - C$ relations for relativistic stars in $f(Q)$ gravity

Muhammad Azzam Alwan <sup>a,b</sup> Tomohiro Inagaki <sup>a,c,d</sup> S.A. Narawade <sup>e</sup> and B. Mishra <sup>e</sup>

<sup>a</sup>Graduate School of Advanced Science and Engineering, Hiroshima University, Higashi-Hiroshima 739-8526, Japan

<sup>b</sup>Research Center for Quantum Physics, National Research and Innovation Agency (BRIN), Tangerang Selatan 15314, Indonesia

<sup>c</sup>Information Media Center, Hiroshima University, Higashi-Hiroshima 739-8521, Japan

<sup>d</sup>Core of Research for the Energetic Universe, Hiroshima University, Higashi-Hiroshima 739-8526, Japan

<sup>e</sup>Department of Mathematics, Birla Institute of Technology and Science-Pilani, Hyderabad Campus, Hyderabad-500078, India.

E-mail: [azzam-alwan@hiroshima-u.ac.jp](mailto:azzam-alwan@hiroshima-u.ac.jp), [inagaki@hiroshima-u.ac.jp](mailto:inagaki@hiroshima-u.ac.jp), [shubhamn2616@gmail.com](mailto:shubhamn2616@gmail.com), [bivu@hyderabad.bits-pilani.ac.in](mailto:bivu@hyderabad.bits-pilani.ac.in)

**Abstract.** We investigate the properties of neutron stars within the framework of  $f(Q)$  gravity by incorporating rotational effects through a slowly rotating metric, extending previous work. We derive the modified TOV equations and calculate the angular velocity profiles and moments of inertia for linear, quadratic, logarithmic, and exponential  $f(Q)$  models. Our results show that deviations in the moment of inertia are more pronounced than those in the maximum mass, providing a strong constraint for alternative gravity theories. We also find a universal relation between the dimensionless moment of inertia and compactness, which shows distinct deviations from GR in  $f(Q)$  models. Additionally, we analyze hybrid and quark star EoS, demonstrating consistency with the behavior observed in the calculation of the  $\bar{I} - C$  relation for PSR J0737-3039A, which could be explored further and is interesting for future studies. Our findings suggest that  $f(Q)$  gravity offers the possibility of being tested in the strong-field regime by examining the properties of compact objects and constraining the  $f(Q)$  parameters through universal relations, such as the  $I - C$  relation, in potential future observations.

**Keywords:**  $f(Q)$  gravity, neutron stars, slowly rotating metric,  $\bar{I} - C$  relation

---

## Contents

<b>1</b>	<b>Introduction</b>	<b>1</b>
<b>2</b>	<b>Mathematical Framework</b>	<b>3</b>
2.1	Basic $f(Q)$ Formalism	3
2.2	Numerical Setup	4
<b>3</b>	<b>Impact of <math>f(Q)</math> models on Slowly Rotating case</b>	<b>8</b>
3.1	Moment of Inertia	8
3.2	Universal $\bar{I} - C$ Relation	11
<b>4</b>	<b>Conclusion</b>	<b>14</b>
<b>A</b>	<b>Fitting Coefficients from the best-fit of each model</b>	<b>16</b>

---

## 1 Introduction

General Relativity (GR) has been proven to be a successful theory [1], extensively tested across wide range of environments. These include weak-field scenarios such as the Solar System and laboratory experiments [2] to strong-field regimes, where the prediction and observation of Gravitational Waves (GW) are involved [3–5]. The GWs detected by LIGO and Virgo are waves produced by the interaction of two compact objects in astrophysics, such as black holes (BH) and neutron stars (NS), which are high-density objects with extreme gravitational environments. The first GW detection, GW150914 [6], was produced by a black hole merger. This event not only provided strong support for GR, but also opened up the opportunity to test gravity under extreme conditions, where deviations from GR can occur, allowing for the testing of alternative theories of gravity. However, testing gravity through black holes has limitations, mainly because of the difficulty in obtaining observational data. Unlike black holes, neutron stars have abundant observational data and have interior structures rich in matter such as degenerate neutrons or various exotic materials, such as hyperons, quarks, or pion condensates, making them ideal astrophysical objects to test gravity in strong fields [7].

One approach to calculate the properties of a neutron star is by solving the Tolman-Oppenheimer-Volkoff (TOV) equation, incorporating a given Equation of State (EoS), and then comparing the results with observational constraints. For example, the results from GW observations of a compact binary coalescence, suspected to involve a neutron star, GW190425 [5], provide a neutron star mass constraint of up to  $2.59 \pm 0.08 M_{\odot}$ . Similarly, pulsar observations of PSR J2215+5135 [8] by the Neutron Star Interior Composition Explorer (NICER) give a neutron star mass of  $2.27^{+0.17}_{-0.15} M_{\odot}$ . These measurements have ruled out many soft EoS, as they cannot align their predictions with the observed neutron star

mass. Furthermore, the discovery of the double-pulsar system PSR J0737-3039 [9, 10] provides another constraint on the EoS through the calculation of the moment of inertia of the PSR J0737-3039 A neutron star [11, 12]. However, using modified gravity theories, the predictions of GR deviate, offering an alternative where previously ruled-out EoS can match observed properties, such as higher or lower masses for stiff EoS [13–19]. Amid this EoS uncertainty, Yagi and Nunes (2013) introduced the universal relation, the relations between several dimensionless quantities that are weakly dependent on the EoS [20]. This relation reveals a common pattern, even though the interaction between gravity and matter may vary in each EoS, thus providing a new perspective on testing theories in the strong-field regime. Various modifications of gravity have been studied to examine how they deviate from different universal relations in neutron stars, rather than due to changes in the EoS [21–26]. This, of course, would serve as a valuable tool for testing both GR and alternative theories of gravity. In this paper, we will explore a universal relation for neutron stars within the  $f(Q)$  gravity framework.

One of the main drivers of modified gravity research is the cosmological constant problem and the elusive nature of dark energy [27–31]. The  $f(Q)$  theories represent a natural extension of Einstein’s GR and have gained significant attention as alternative gravity theories, particularly for explaining the accelerated expansion of the universe. These theories involve modifying the standard Einstein-Hilbert Lagrangian, replacing it with a function of the Non-metricity scalar  $Q$ . Various classes of  $f(Q)$  theories have been explored, and many models have been constructed and analyzed (for a detailed review, see [32–37, 37]). While  $f(Q)$  theories are primarily applied to cosmological phenomena [38–43], they also have important implications for astrophysical objects. In the context of  $f(Q)$  gravity, compact objects have been studied extensively in the literature [44–50]. In our previous study [46], we examined how the interior geometry of neutron stars is influenced by non-metricity under static condition, which subsequently affects their density, pressure, and stability. Deviations arising from modifications of  $f(Q)$  can enable stars to accommodate more matter, increasing their mass, or lead to a loss of stability, causing them to become lighter or even collapse. In one of the  $f(Q)$  models, we observed maximum mass deviations that could accommodate EoS like APR4, aligning with various observational constraints from pulsar and gravitational wave observations. Building on these results, we extended our study to neutron stars in  $f(Q)$  gravity in the slowly rotating case, employing 9 different EoS. In this case, the additional effect of rotation enables us to derive moment of inertia properties that cannot be obtained in the static case. From various references on other modified gravity theories, we expect that  $f(Q)$  models can cause deviations in the angular velocity ( $\bar{\omega}_c$ ) at the center of neutron stars, resulting in greater deviations in the moment of inertia compared to our previous calculations in the mass-radius diagram. Through the moment of inertia, we also calculate one of the universal relations between the dimensionless moment of inertia ( $\bar{I}$ ) and the compactness of stars ( $C$ ). Based on the differences in  $\bar{\omega}_c$  values, we anticipate obtaining a  $\bar{I} - C$  relation with a shape similar to that of GR, but shows different deviation between each model which shows their respective signatures. From these calculations, we expect this relationship to serve as a constraint on the  $f(Q)$  parameter through possible

future measurements.

This paper is organized as follows: In Section 2, we introduce the mathematical framework of  $f(Q)$  gravity, along with the numerical setup, which includes the step to solve the field equations and the selection of the EoS. Section 3 focuses on analyzing the impact of  $f(Q)$  models on the properties of slowly rotating neutron stars, particularly focusing on the moment of inertia. In this section, we also investigate the universal  $\bar{I} - C$  relation, computing and fitting it across various  $f(Q)$  models. Finally, we summarize our findings and outline potential future directions in Section 4.

## 2 Mathematical Framework

### 2.1 Basic $f(Q)$ Formalism

In a spacetime characterized by a metric tensor  $g_{\mu\nu}$  and an affine connection  $\Gamma^\lambda_{\mu\nu}$ , the torsion tensor  $T^\lambda_{\mu\nu}$  and the non-metricity tensor  $Q_{\lambda\mu\nu}$  are defined as,

$$T^\lambda_{\mu\nu} := \Gamma^\lambda_{\mu\nu} - \Gamma^\lambda_{\nu\mu}, \quad Q_{\lambda\mu\nu} := \nabla_\lambda g_{\mu\nu} = \partial_\lambda g_{\mu\nu} - \Gamma^\alpha_{\lambda\mu} g_{\alpha\nu} - \Gamma^\alpha_{\lambda\nu} g_{\alpha\mu}. \quad (2.1)$$

The decomposition of the general affine connection allows us to clearly distinguish the contributions from torsion and non-metricity, separating them from the purely metric-compatible component of the connection. This can be represented as the sum of the Levi-Civita connection  $\left(\left\{\overset{\lambda}{\mu\nu}\right\}\right)$ , contortion  $\left(K^\lambda_{\mu\nu}\right)$ , and disformation  $\left(L^\lambda_{\mu\nu}\right)$ . This relationship can be expressed mathematically as,

$$\Gamma^\lambda_{\mu\nu} = \left\{\overset{\lambda}{\mu\nu}\right\} + K^\lambda_{\mu\nu} + L^\lambda_{\mu\nu}, \quad (2.2)$$

where

$$\left\{\overset{\lambda}{\mu\nu}\right\} = \frac{1}{2}g^{\lambda\alpha} \left(\partial_\mu g_{\alpha\nu} + \partial_\nu g_{\alpha\mu} - \partial_\alpha g_{\mu\nu}\right), \quad K^\lambda_{\mu\nu} = \frac{1}{2} \left(T^\lambda_{\mu\nu} + T_\mu^{\lambda\nu} + T_\nu^{\lambda\mu}\right), \\ L^\lambda_{\mu\nu} = \frac{1}{2} \left(Q^\lambda_{\mu\nu} - Q_\mu^{\lambda\nu} - Q_\nu^{\lambda\mu}\right).$$

A modified  $f(Q)$  theory of gravity with symmetric teleparallelism considers an affine connection with vanishing curvature and null torsion and let non-metricity be the only driving force. The non-metricity scalar is defined as [32],

$$Q = Q_{\lambda\mu\nu} P^{\lambda\mu\nu} = \frac{1}{4} \left( -Q_{\lambda\mu\nu} Q^{\lambda\mu\nu} + 2Q_{\lambda\mu\nu} Q^{\mu\nu\lambda} + Q_\lambda Q^\lambda - 2Q_\lambda \tilde{Q}^\lambda \right). \quad (2.3)$$

where  $Q_\lambda = g^{\mu\nu} Q_{\lambda\mu\nu}$ ,  $\tilde{Q}^\lambda = g^{\mu\nu} Q_{\mu\nu\lambda}$  are two traces of non-metricity tensor and its conjugate  $P^\lambda_{\mu\nu}$  is called as superpotential, given by

$$P^\lambda_{\mu\nu} = -\frac{1}{4} Q^\lambda_{\mu\nu} + \frac{1}{4} \left( Q_\mu^{\lambda\nu} + Q_\nu^{\lambda\mu} \right) + \frac{1}{4} Q^\lambda g_{\mu\nu} - \frac{1}{8} \left( 2\tilde{Q}^\lambda g_{\mu\nu} + \delta_\mu^\lambda Q_\nu + \delta_\nu^\lambda Q_\mu \right). \quad (2.4)$$

The non-metricity scalar  $Q$  is invariant under local general linear transformations and translational symmetries. An alternative definition found in the literature,  $Q = -Q_{\lambda\mu\nu} P^{\lambda\mu\nu}$ ,

results in a sign change for the scalar. This is important when comparing different  $f(Q)$  results. Additionally, the non-metricity scalar  $Q$  can replace the Ricci scalar  $R$  in the Einstein-Hilbert action, yielding the symmetric teleparallel equivalent of General Relativity (GR), known as STEGR. It is noteworthy that symmetric teleparallel theory faces the same 'dark' problem as conventional GR. Modified gravity theories of the form  $f(Q)$  were developed to address these issues, in a similar way to the extensions seen in modified gravity theories represented by  $f(R)$ .

The components of the connection in Eq. (2.2) can be rewritten as,

$$\Gamma^\lambda{}_{\mu\beta} = \frac{\partial y^\lambda}{\partial \tilde{\zeta}^\rho} \partial_\mu \partial_\beta \tilde{\zeta}^\rho. \quad (2.5)$$

In the given equation, the relation  $\tilde{\zeta}^\lambda = \zeta^\lambda(y^\mu)$  is invertible, and  $\frac{\partial y^\lambda}{\partial \tilde{\zeta}^\rho}$  is the inverse of the corresponding Jacobian matrix [51]. This scenario is referred to as a coincident gauge, where it is always possible to select a coordinate system in which the connection coefficients  $\Gamma^\lambda{}_{\mu\nu}$  vanish. In this gauge, the covariant derivative  $\nabla_\lambda$  simplifies to the partial derivative  $\partial_\lambda$  leading to the expression  $Q_{\lambda\mu\nu} = \partial_\lambda g_{\mu\nu}$ . Therefore, the Levi-Civita connection  $\left(\left\{\begin{smallmatrix} \lambda \\ \mu\nu \end{smallmatrix}\right\}\right)$  can be rewritten in terms of the disformation tensor  $L^\alpha{}_{\mu\nu}$  as  $\left(\left\{\begin{smallmatrix} \lambda \\ \mu\nu \end{smallmatrix}\right\}\right) = -L^\lambda{}_{\mu\nu}$ . By varying the action term [32, 52]

$$S = \int \frac{1}{2\kappa} f(Q) \sqrt{-g} d^4x + \int \mathcal{L}_m \sqrt{-g} d^4x, \quad (2.6)$$

with respect to the metric tensor, we can obtain the field equation

$$\frac{2}{\sqrt{-g}} \nabla_\lambda \left( \sqrt{-g} f_Q P^\lambda{}_{\mu\nu} \right) - \frac{1}{2} g_{\mu\nu} f + f_Q (P_{\mu\lambda\alpha} Q_v{}^{\lambda\alpha} - 2Q_{\lambda\alpha\mu} P^{\lambda\alpha}{}_\nu) = \kappa \mathcal{T}_{\mu\nu}. \quad (2.7)$$

Using this field equation, the covariant formulation has been developed and used effectively in studying geodesic deviations and cosmological phenomena [52–55],

$$f_Q \mathring{G}_{\mu\nu} + \frac{1}{2} g_{\mu\nu} (Q f_Q - f) + 2f_{QQ} P^\lambda{}_{\mu\nu} \mathring{\nabla}_\lambda Q = \kappa \mathcal{T}_{\mu\nu}, \quad (2.8)$$

where,  $f_Q$  is derivative of  $f$  with respect to  $Q$  and  $\mathring{G}_{\mu\nu} = R_{\mu\nu} - \frac{1}{2} g_{\mu\nu} R$ , with  $R_{\mu\nu}$  and  $R$  are the Riemannian Ricci tensor and scalar respectively which are constructed by the Levi-Civita connection. For a linear form of  $f(Q)$  function, the above equation reduces to GR. Variation of Eq. (2.4) with respect to the connection, we can derive the equation of motion for the nonmetricity scalar as,

$$\nabla_\mu \nabla_\nu \left( \sqrt{-g} f_Q P^{\mu\nu}{}_\lambda \right) = 0. \quad (2.9)$$

## 2.2 Numerical Setup

We have developed a modified TOV equation for non-rotating neutron stars in covariant  $f(Q)$  gravity across several models, providing profiles and properties in our previous work

[46]. Now, we will calculate slowly rotating neutron stars by incorporating rotational terms as [22, 56, 57]

$$ds^2 = -e^{A(r)}dt^2 + e^{B(r)}dr^2 + r^2d\theta^2 + r^2\sin^2\theta d\phi^2 - 2\omega(r)\epsilon r^2\sin^2\theta dt d\phi, \quad (2.10)$$

This metric describes the spacetime geometry with a rotational term,  $\omega(r)$ , where  $\omega(r)$  represents the angular velocity of the inertial frame dragged by the rotation of star. The parameter  $\epsilon$  in the  $\omega$  term denotes slow rotation, where  $\epsilon$  must be small,  $\epsilon \ll 1$ . When  $\epsilon$  equals zero, we recover the static and spherically symmetric metric. Now, by eliminating the parameters that contain information of gravity in the metric Eq. (2.10), we can achieve a flat, curvature-free spacetime by simply setting  $A(r) = 0$ ,  $B(r) = 0$ , and  $\epsilon = 0$ . This reduces the metric to the Minkowski metric in spherical coordinates:

$$ds^2 = -dt^2 + dr^2 + r^2d\theta^2 + r^2\sin^2\theta d\phi^2, \quad (2.11)$$

and denoted by  $\mathcal{G}_{(r)}$ . Our next step is to determine which affine connection best fits the spacetime determined by the metric  $\mathcal{G}_{(r)}$ . Further, it is well known in GR that gravity in Minkowski spacetime Eq. (2.11) is represented by the curvature tensor  $\mathring{R}_{(r)\mu\nu\rho}{}^\sigma$  and in STEGR theory, it is represented by the non-metricity tensor  $Q_{(r)\lambda\mu\nu}$ , so it is meaningful to assume  $Q_{(r)\lambda\mu\nu} = 0$  for the new spacetime determined by  $\mathcal{G}_{(r)}$ . Based on this assumption and Levi-Civita connection Eq. (2.2), we can calculate the non-vanishing components of arbitrary affine connections:

$$\begin{aligned} \Gamma_{r\theta}^\theta &= \Gamma_{\theta r}^\theta = \Gamma_{r\phi}^\phi = \Gamma_{\phi r}^\phi = \frac{1}{r}, & \Gamma_{\theta\theta}^r &= -r \\ \Gamma_{\phi\theta}^\phi &= \Gamma_{\theta\phi}^\phi = \cot\theta, & \Gamma_{\phi\phi}^r &= -r\sin^2\theta, & \Gamma_{\phi\phi}^\theta &= -\cos\theta\sin\theta. \end{aligned} \quad (2.12)$$

Using the metric Eq. (2.10) and connection Eq. (2.12), we can get the equations of motion of  $f(Q)$  theory for slowly rotating spherically symmetric metric for first order  $\mathcal{O}(\epsilon)$ ,

$$\begin{aligned} \kappa\mathcal{T}_{tt} &= \frac{e^{A-B}}{2r^2} \left\{ r^2e^B f + 2f'_Q r(e^B - 1) + f_Q \left[ (e^B - 1)(2 + rA') + (1 + e^B)rB' \right] \right\}, \\ \kappa\mathcal{T}_{rr} &= \frac{-1}{2r^2} \left\{ r^2e^B f + 2f'_Q r(e^B - 1) + f_Q \left[ (e^B - 1)(2 + rA' + rB') - 2rA' \right] \right\}, \\ \kappa\mathcal{T}_{\theta\theta} &= -\frac{r}{4e^B} \left\{ f_Q \left[ -4A' - r(A')^2 - 2rA'' + rA'B' + 2e^B(A' + B') \right] + 2e^B r f - 2f'_Q r A' \right\}, \\ \kappa\mathcal{T}_{t\phi} &= \frac{1}{4} r \epsilon e^{-B} \sin^2(\theta) \left\{ 2f_Q r \omega'' - \left( f_Q (rA' + rB' - 8) - 2r f'_Q \right) \omega' + \left( 2f'_Q (-rA' + e^B + 1) \right. \right. \\ &\quad \left. \left. + f_Q A' (rB' + 2e^B - 4) + 2 \left( -f_Q r A'' + f_Q e^B B' + f r e^B \right) - f_Q r A'^2 \right) \omega \right\}. \end{aligned} \quad (2.13)$$

As noticed from Eq. (2.13), the field equations for the diagonal components remain unchanged. However, the inclusion of rotation introduces an additional field equation arising

from the  $t\phi$  component. In the slowly rotating case, the non-metricity tensor retains a similar form at  $\mathcal{O}(\epsilon)$ . Assuming the star is composed of a perfect fluid with a given EoS, the energy-momentum tensor is expressed as

$$\mathcal{T}_{\mu\nu} = (\rho + p)u_\mu u_\nu + p g_{\mu\nu} \quad (2.14)$$

where the four-velocity components are

$$u^r = u^\theta = 0, \quad u^\phi = \Omega u^t, \quad u^t = \left[ - (g^{tt} + 2\Omega g^{t\phi} + \Omega^2 g^{\phi\phi}) \right]^{1/2}$$

The field equations Eq. (2.13) can then be written as a set of equations that include the Tolman-Oppenheimer-Volkov (TOV) equations for  $f(Q)$  gravity, describing the internal structure of neutron stars, as shown in [46] as

$$\begin{aligned} A'' &= \frac{2e^B \left( r(f(Q) + 2p\kappa) + f_Q (A' + B') \right) - A' \left( f_Q (4 + rA' - rB') + 2f_{QQ}rQ' \right)}{2f_Q r}, \\ B' &= \frac{-\kappa e^B (p + \rho)r + f_Q A'}{f_Q}, \\ p' &= -\frac{(p + \rho)}{2} A'. \end{aligned} \quad (2.15)$$

An additional equation is obtained from the non-diagonal field equation that provides the angular velocity profile of the star as

$$\begin{aligned} \bar{\omega}'' &= f_2(A', B', Q', Q, r)\bar{\omega}' + f_1(A'', A', B', B, Q', Q, r, \rho)\bar{\omega} + f_0(A'', A', B', B, Q', Q, r, \rho, p), \\ f_2 &= \frac{f_Q r (A' + B') - 2r f_Q' - 8f_Q}{2f_Q r}, \\ f_1 &= \frac{2f_Q r A'' - 2e^B \left( f_Q (A' + B') + r(f(Q) - 16\pi\rho) \right)}{2f_Q r} \\ &\quad + \frac{f_Q A' (rA' - rB' + 4) - 2f_Q' \left( -rA' + e^B + 1 \right)}{2f_Q r}, \\ f_0 &= \frac{-2f_Q r A'' - f_Q (A' - B') (rA' + 2) + 2e^B r(f(Q) - f_Q Q + 16\pi p) + 2 \left( e^B + 1 \right) f_{QQ} Q'}{2f_Q r}. \end{aligned} \quad (2.16)$$

Here,  $\bar{\omega} := \Omega - \omega(r)$  represents the difference between the angular velocity  $\Omega$  observed by a free-falling observer at infinity and the angular velocity of a fluid element measured by a local stationary observer within the fluid and  $\Omega$  is spin frequency. In this context, we rescale  $\bar{\omega}$  by defining the normalized metric function  $\bar{\omega}/\Omega$  as a function of the radial coordinate, which makes the equations dimensionless.

From this, we can observe that the system of equations in Eq. (2.15) and Eq. (2.16) is separable, where the presence of the equation for  $\bar{\omega}$  does not change Eq. (2.15). This holds only at  $\mathcal{O}(\epsilon)$ . At  $\mathcal{O}(\epsilon^2)$ , this no longer applies, and the resulting equations become more complex. From Eq. (2.15) and Eq. (2.16), we can obtain the solution of these TOV ODEs by integrating the equations from the center of the star outward. At the surface of the star,  $\bar{\omega}$  has a boundary condition given by

$$\bar{\omega} = 1 - \frac{2J/\Omega}{r^3}, \quad (2.17)$$

where  $J$  is the total angular momentum of the star, and the moment of inertia is given by  $I = J/\Omega$ . In the exterior region of the star, Eq. (2.16) simplifies to

$$\bar{\omega}'' - \frac{4\bar{\omega}'}{r} = 0, \quad (2.18)$$

which same with the form found in [56]. The solutions of these interior and exterior equations must match at the boundary condition Eq. (2.17). Once this is done, we can extract the value of the moment of inertia, which is derived as

$$I := \frac{J}{\Omega} = \frac{R^4}{6\Omega} \left( \frac{d\bar{\omega}}{dr} \right)_R, \quad (2.19)$$

where  $R$  is the radius of the star at the surface. Furthermore, at the surface of the star, the pressure approaches zero, allowing us to define the boundary value as

$$p(R) \approx 0. \quad (2.20)$$

For the non-metricity, according to the formulation of covariant  $f(Q)$ , the condition  $A' + B' = 0$  in vacuum leads to  $Q(r) = 0$  outside the star. This can be readily obtained by evaluating Eq. (2.13). Using the relations  $A'(r) + B'(r) = 0$  and  $e^{A(r)} = e^{-B(r)}$ , which are easily derived from Eq. (2.13), the exterior solution of the star can be written as:

$$e^{-B(r)} = e^{A(r)} = 1 + \frac{C}{r} + \frac{f(Q)|_0}{6f_{Q|0}} r^2, \quad (2.21)$$

where  $C$  is an integration constant. This solution resembles the Schwarzschild-de Sitter (SdS) solution with the cosmological constant  $\Lambda = \frac{f(Q)|_0}{2f_{Q|0}}$ . The transition from the interior to the exterior of the star must satisfy the junction conditions discussed in our previous work [46]. After determining the boundary values of the system, we require initial values for each variable to solve these ODEs. In this discussion, we use the following initial values:

$$B = 0, \quad A' = 0, \quad A = A_0, \quad Q = 0, \quad p = p_c, \quad \bar{\omega}' = 0, \quad \bar{\omega} = \bar{\omega}_c, \quad (2.22)$$

where  $\bar{\omega}_c$  and  $A_0$  is a constant that can be chosen arbitrarily and will later be matched with the boundary condition at the star's surface using the shooting method. Meanwhile,  $p_c$  is the pressure at the center of the star, which serves as a parameter when solving the ODEs using EoS.



To solve these ODEs, we also need to use dimensionless physical variables, defined as

$$\hat{r} = \frac{r}{r_g}, \quad \hat{p} = \frac{p}{p_g}, \quad \hat{\rho} = \frac{\rho}{\rho_g}, \quad \hat{Q} = Qr_g^2, \quad \hat{m} = \frac{m}{M_\odot}, \quad (2.23)$$

where

$$r_g = \frac{GM_\odot}{c^2}, \quad p_g = \frac{M_\odot c^2}{r_g^3}, \quad \rho_g = \frac{M_\odot}{r_g^3}. \quad (2.24)$$

In this context,  $M_\odot$  represents the mass of the Sun,  $c$  is the speed of light, and  $G$  is the gravitational constant. These constants are expressed in the cgs unit system, where  $M_\odot \approx 1.989 \times 10^{33}$  g,  $c \approx 2.997 \times 10^{10}$  cm/s, and  $G \approx 6.674 \times 10^{-8}$  dyne cm<sup>2</sup>/g<sup>2</sup>. Note that  $\bar{\omega}$  is not rescaled, as it is already normalized by  $\Omega$ . With this setup, we can compute the profiles of the neutron star, particularly  $\bar{\omega}$  and the moment of inertia as properties of the NS, which will be discussed further in this paper. Using some realistic EoS, we apply the Runge-Kutta method available in the `scipy.integrate.solve_ivp` package in python to numerically integrate the ODEs and obtain the solutions. This package provides a flexible and computationally efficient approach for solving initial value problems in ODEs.

### 3 Impact of $f(Q)$ models on Slowly Rotating case

Using the TOV equations and the numerical setup discussed in the previous section, we calculate the profile of  $\bar{\omega}$  and the properties of the neutron star that can be obtained in the slowly rotating case, specifically the moment of inertia. From the results, we can compute the universal  $\bar{I} - C$  relation and demonstrate the deviations of various  $f(Q)$  models from this relation, independent of the EoS. In this section, we analyze the rotation effects in the extended  $f(Q)$  gravity using several models, specifically the linear, quadratic, exponential, and logarithmic models, given by,

$$f(Q) = \alpha_1 Q + \beta_1, \quad f(Q) = Q + \alpha_2 Q^2, \quad f(Q) = Q + \alpha_3 e^{\beta_3 Q}, \quad f(Q) = Q - \alpha_4 \ln(1 - \beta_4 Q), \quad (3.1)$$

where  $\alpha$  and  $\beta$  are model parameters. The non-linear  $f(Q)$  models have been extensively explored in our previous work [46]. Additionally, this paper examines the linear  $f(Q)$  model, which has been widely studied in the context of compact star scenarios [48–50, 58]. However, the linear model in this case is slightly different because we consider an isotropic fluid, not anisotropic, as the matter inside the neutron star. By using the assumption of the contracted energy-momentum conservation  $\nabla^\mu \mathcal{T}_{\mu\nu} = 0$ , we obtain the condition where  $f_{QQ} = 0$ . In this model,  $\alpha_1$  is a constant of integration from the  $f_{QQ} = 0$  condition, and  $\beta_1$  is a constant of integration from  $f_Q$ , resulting in the linear form  $f(Q) = \alpha_1 Q + \beta_1$ .

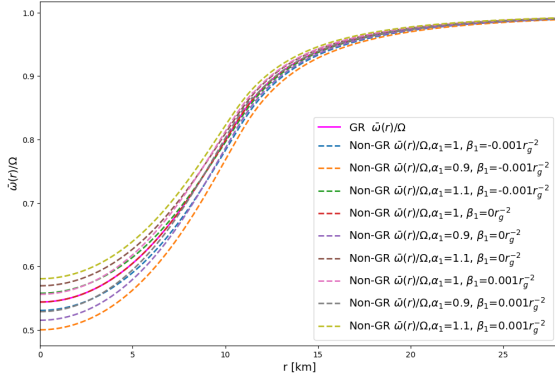
#### 3.1 Moment of Inertia

Utilizing the numerical framework outlined in Sec. 2.2, we calculate the  $\bar{\omega}$  profiles for each model, as illustrated in Fig. 1. This figure presents  $\bar{\omega}$  normalized by  $\Omega$  for different values for each model, employing the SLy EoS [59]. To determine the surface of the star, we set the condition  $p(R) \leq 10^{-8} p_c$ . At  $\rho = 1 \times 10^{15}$ , the models exhibit noticeable deviations from

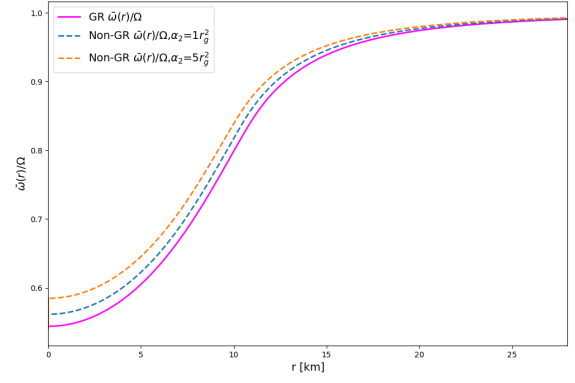
GR. Each model utilizes distinct initial values of  $\bar{\omega}$ , which are calibrated through the shooting method to satisfy the exterior boundary conditions specified at the surface of the star, as given in Eq. (2.18). This indicates that the deviations become stronger toward the center of the star, potentially due to the influence of non-metricity. As one moves outward from the origin, the deviations from the central conditions gradually decrease, approaching the asymptotic condition at infinity, where the ratio  $\bar{\omega}/\Omega$  converges to 1. As anticipated from our prior analysis, smaller values of  $\rho_c$  lead to smaller deviations from GR, which become almost negligible. Conversely, larger values of  $\rho_c$  cause stronger deviations from GR, aligning with the observed characteristics of neutron star configurations within the framework of covariant  $f(Q)$  gravity [46]. Changing the parameters  $\alpha$  and  $\beta$  can effectively reduce the deviations in the central values of  $\bar{\omega}$ . By decreasing these parameter values, the results can approach or even coincide with the GR. This is evident in Fig. 1a, where for  $\alpha_1 = 1$  and  $\beta_1 = 0$ , the graph aligns perfectly with GR, indicating that the TOV equations revert to the GR case.

One of the concerns with the  $\bar{\omega}$  profiles is the behavior of the exponential model. In this model, we only use values of  $\alpha_3 = \pm 0.001$  and  $\pm 0.01$ , since larger deviations in  $\bar{\omega}$  are observed when  $\alpha_3 = 0.1$ . For example, when  $\alpha_3 = \pm 0.01$ , the difference in  $\bar{\omega}_c$  compared to GR ranges from 5.2% to 5.9%. However, at  $\alpha_3 = \pm 0.1$ , the deviations become much more pronounced, reaching 32% for  $\alpha_3 = -0.1$  and 210% for  $\alpha_3 = 0.1$ . These results suggest that the rotational effects in the exponential model can lead to substantial deviations, potentially making neutron stars less stable. This is further supported by the  $\bar{I} - C$  relation, which is discussed later. This result differs from our previous work, where values of  $\alpha_3$  ranging from 0.1 to 1 produced noticeable yet stable deviations in the mass-radius relation, indicating a potential limitation of the exponential model for slowly rotating stars. Additionally, the parameter  $\beta_3$  in this model seems to have minimal effects on the  $\bar{\omega}$  profile. In earlier studies, values of  $\alpha_3 = 0.1$  with  $\beta_3 = 0.1$  and  $\beta_3 = 0.5$  led to a maximum mass difference of up to 6.8%. This discrepancy might arise because the value of  $\alpha$  in the current analysis is too small, making the fine-tuning effect of  $\beta$  negligible. For other models, such as linear, quadratic, and logarithmic, the differences in  $\bar{\omega}_c$  range from 2.7% to 12.3%. Although the logarithmic model, for example, shows differences as large as 12.3%, the resulting neutron stars remain stable and exhibit similar behavior when the parameters  $\alpha_4$  and  $\beta_4$  are varied, consistent with our previous work. In the linear model of  $f(Q)$ , where  $\beta_1$  serves as the integration constant,  $\beta_1$  proves to be highly sensitive, as it affects the magnitude of  $f(Q)$ , which in turn impacts the stability of the star. Thus, in our numerical calculations, we used very small values for  $\beta_1$ . On the other hand,  $\alpha_1$  is more flexible as it scales  $Q$ .

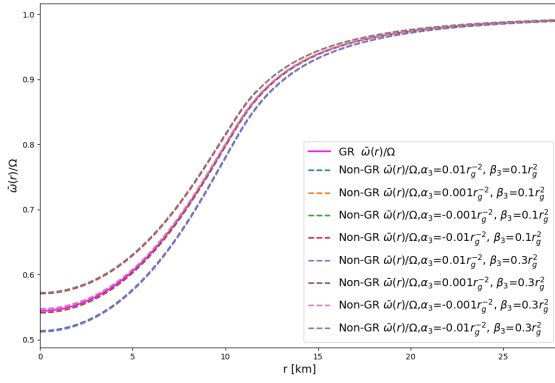
After calculating the  $\bar{\omega}$  profiles for each model, we proceed to compute the moment of inertia using the values of  $\bar{\omega}$  at the surface, as given by Eq. (2.19). In Fig. 2, we plot the moment of inertia of the neutron star as a function of its mass for each model, with different parameter values. The results are consistent with our previous calculations of  $\bar{\omega}$ , where, as the parameters approach zero, the moment of inertia converges to the value predicted by GR. If we observe the moment of inertia of all models at low masses, the moment of inertia of the neutron star closely matches the GR result, except for the linear and the



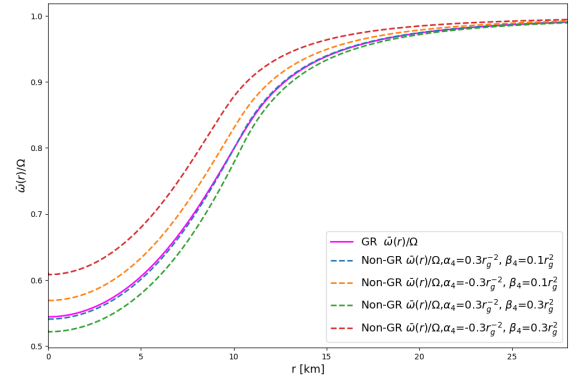
(a)  $\bar{\omega}/\Omega$  profile of  $f(Q) = \alpha_1 Q + \beta_1$



(b)  $\bar{\omega}/\Omega$  profile of  $f(Q) = Q + \alpha_2 Q^2$



(c)  $\bar{\omega}/\Omega$  profile of  $f(Q) = Q + \alpha_3 e^{\beta_3 Q}$



(d)  $\bar{\omega}/\Omega$  profile of  $f(Q) = Q - \alpha_4 \ln(1 - \beta_4 Q)$

**Figure 1:** The normalized  $\bar{\omega}/\Omega$  profile as a function of radius, computed using the SLy4 EoS at a density of  $\rho = 1 \times 10^{15}$  g/cm<sup>3</sup>. For each model, various values of  $\alpha$  and  $\beta$  are considered. By applying the matching condition between the interior and exterior solutions, different initial values are determined for each parameter, highlighting the deviations of each  $f(Q)$  model from GR. In this graph, the star surface radius in GR is approximately 11.7 km.

exponential model. In the models, the largest deviation reaches  $\sim 20\%$  at low mass. This reinforces the presumption that the rotational effects significantly affect the stability of neutron stars obtained in the exponential model. Although other references, such as [60], show that the moment of inertia exhibits larger deviations than the maximum mass deviation, in this model, the deviations are so large that we can only calculate for small values of  $\alpha$  up to the order of  $\mathcal{O}(10^{-2})$  for exponential model and  $\mathcal{O}(10^{-3})$  for linear model. Another possible explanation is that if we expand the exponential term using a Taylor series, we can obtain  $f(Q) = Q + \alpha_3(1 + \beta_3 Q + \frac{\beta_3^2 Q^2}{2} + \mathcal{O}(Q^3))$ , where  $\alpha_3$  and  $\beta_3$  represent terms that are part of the exponential expansion. There is a similarity with the linear model  $f(Q)$ , where the term  $\alpha_3$  in this case plays the role of  $\beta_1$  in linear  $f(Q)$ , and the term  $\alpha_3 \beta_3 Q$  will become an additional linear  $Q$ -term, similar to  $\alpha_1 Q$  in the linear  $f(Q)$ . The quadratic term becomes so small that it can be neglected. If we compare  $\alpha_3$  and  $\beta_1$ , we can observe that both models

only achieve stable moments of inertia at small maximum mass deviations, particularly at orders around  $10^{-3}r_g^{-2}$ . This suggests that for the slowly rotating case, both models can only stabilize neutron stars when the maximum mass deviation is small, as can be seen in Fig. 2a and 2c. For the quadratic model, the maximum deviation occurs at  $\alpha_2 = 5r_g^2$ , with a deviation of approximately  $\sim 49\%$ . We tested various values of  $\alpha_2 = 10, 50, 10^2, 10^3, 10^4 r_g^2$  and observed that the maximum deviation in the moment of inertia decreases with  $\alpha_2 > 5r_g^2$ . We also found that the moment of inertia tends to stagnate at  $\alpha_2 = 10^2 r_g^2$ , which is lower than the corresponding parameter value in quadratic  $f(R) = R + \gamma R^2$  gravity, where stagnation occurs at  $\gamma = 10^4 r_g^2$  [60]. Unfortunately, there are currently no observational constraints on the quadratic  $f(Q)$  parameter. In contrast,  $f(R)$  gravity has a constraint of  $\gamma \gtrsim 2.3 \times 10^5$  [61], derived from the Gravity Probe B experiment. The logarithmic models exhibit similar behavior, where the deviations exceed the maximum mass deviation. However, they demonstrate greater stability compared to the exponential model, particularly for parameters that achieve significantly higher maximum masses.

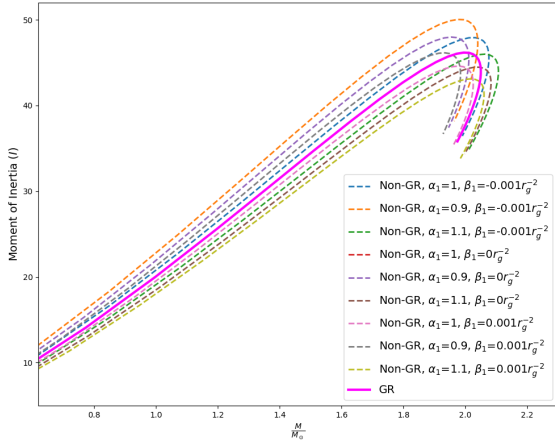
### 3.2 Universal $\bar{I} - C$ Relation

After obtaining the characteristics of the neutron star in the slowly rotating case, including the moment of inertia, we can calculate one of the universal relations, which allows us to derive a connection between the properties of the neutron star without depending on the equation of state used. In this paper, we compute the universal  $\bar{I} - C$  relation, which was first proposed by [62] and comprehensively studied by Breu and Rezzolla [57] in the GR case. The universal  $\bar{I} - C$  relation can be expressed as:

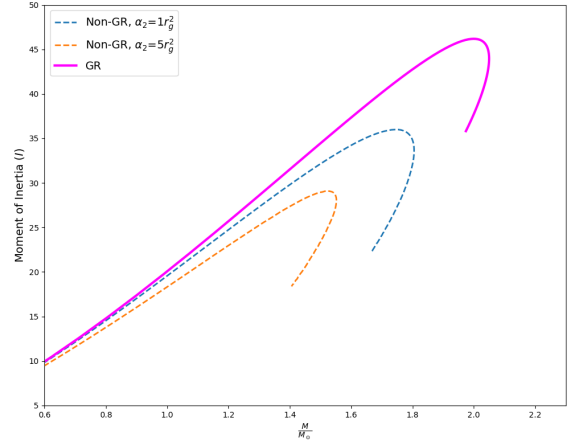
$$I = a_1 C^{-1} + a_2 C^{-2} + a_3 C^{-3} + a_4 C^{-4} . \quad (3.2)$$

where the moment of inertia is normalized to a dimensionless quantity as  $\bar{I} = Ic^2/GM^3$ , and the compactness is defined as  $C = GM/R$ , where  $M$  is the mass of NS,  $R$  is the star surface radius,  $c$  is the speed of light, and  $G$  is the gravitational constant.  $a_{1,\dots,4}$  are fitting coefficients that will be determined through the relationship between these two quantities. In our previous work, we used four EoS - SLy, FPS, AP4, and MS1b - to calculate neutron star profiles and mass-radius properties. In this section, we extend our analysis by employing nine different EoS, seven of which consist solely of normal matter ( $n, p, e, \mu$ ), while two are mixed EoS that include hyperons and quarks. The details of the EoS used are provided in Table 1. In addition to the particle content of these nine EoS, we also consider their stiffness characteristics. For example, FPS belongs to the class of soft realistic EoS, MPA1 represents an intermediate stiffness, and MS1b is categorized as a stiff EoS due to its ability to produce higher maximum masses. We also selected ALF4 because it can model hybrid stars. This selection allows us to explore whether the results can capture the universality of the  $\bar{I} - C$  relation across different particle contents, EoS calculation methods, stiffness levels, and star types, including hybrid stars.

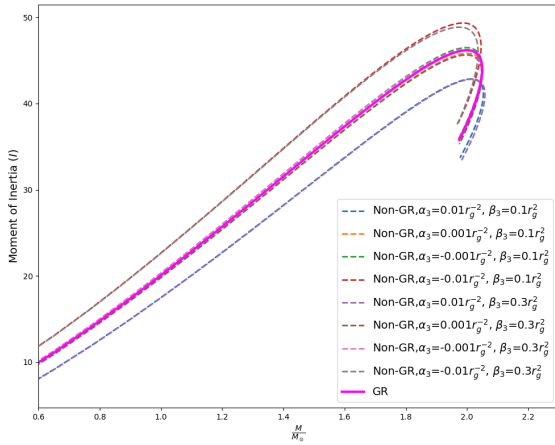
By calculating the moment of inertia, mass, and radius of neutron stars, we successfully computed the universal  $\bar{I} - C$  relation for the four extended  $f(Q)$  gravity models. The



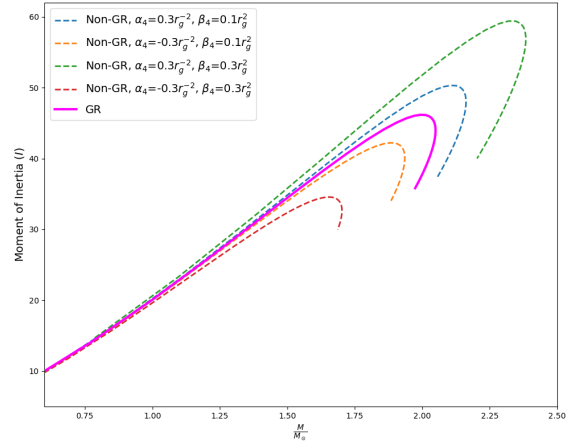
(a) Moment of inertia of  $f(Q) = \alpha_1 Q + \beta_1$



(b) Moment of inertia of  $f(Q) = Q + \alpha_2 Q^2$



(c) Moment of inertia of  $f(Q) = Q + \alpha_3 e^{\beta_3 Q}$



(d) Moment of inertia of  $f(Q) = Q - \alpha_4 \ln(1 - \beta_4 Q)$

**Figure 2:** Moment of inertia as a function of mass for SLy EoS using different values of the parameter  $\alpha$  and  $\beta$  of each model.

results for each model and EoS are shown in Fig. 3. All results demonstrate good universality and are consistent with the relation shown in [57]. In the bottom panels of each graph, we present the residuals from the fitting, defined as  $\Delta = (\bar{I}_{\text{fit}} - \bar{I}) / \bar{I}$ , where all models exhibit a maximum residual of around 10%. We have also explored the EoS with different particle contents, including pions in PS and quarks and hyperons in PCL2 and SQM, which are EoS models for strange stars. In both PCL2 and PS, the calculation results maintain universality. However, the residuals increase by up to 20% at higher compactness due to the dispersion of data points. This may occur, one possible reason being that this EoS is more suitable for anisotropic NS [71–73]. For SQM, the behavior is similar to what is observed in other modified gravity models with changes to the geometric components, such as  $f(R)$  modifications. At low compactness, strange stars deviate from the universal relation, although their  $I$  val-

**Table 1:** The EoS used in our calculations.  $H$  refers to hyperons ( $n, p, \Sigma^\pm, \Sigma^0, \Xi^0, \Xi^-, \Lambda$ ), and  $Q$  refers to quarks ( $u, d, s$ ).

Name	Particle Content	Calculational Method
SLy [59]	$n, p$	Two-potential method
AP4 [63], FPS [64], WFF3 [65]	$n, p$	Eight-variational method
MS1b [66]	$n, p$	Relativistic mean field theory
ENG [67], MPA1 [68]	$n, p$	Nonrelativistic Hartree-Fock method
ALF4 [69]	$n, p, Q$	Eight-variational method
GNH3 [70]	$n, p, H$	Relativistic mean field theory

ues converge toward the neutron star relation at high compactness, indicating the need for further investigation. Therefore, we present the results here without fully considering the characteristics of strange stars at this stage. The best-fit for each model is plotted in Fig. 4 along with its deviation from GR. The calculation results demonstrate consistency with their respective  $\bar{\omega}$  profiles and  $I$  properties. When compared with the mass-radius relation, the  $\bar{I} - C$  relation also shows consistent results. For smaller masses, as observed in the quadratic model or when the additional terms are negative in the logarithmic model, the deviations of  $\bar{I}$  are positive. However, for larger masses, the deviations of  $\bar{I}$  become negative. In contrast, the exponential model exhibits the opposite behavior. When the neutron star has a larger mass, the deviation of  $\bar{I}$  is positive, whereas for smaller masses, the deviation is negative. Indeed, a closer examination reveals that the value of  $\alpha = 0.01r_g^{-2}$  leads to a significantly higher deviation compared to  $\alpha = 0.001r_g^{-2}$  and the GR case. For  $\alpha = 0.01$ , the difference, for instance, when  $C = 0.1$ , reaches 38% and 43% relative to GR. However, at higher compactness, the deviation reduces to just 0.06%. This suggests that observational data on the  $\bar{I} - C$  relation from neutron stars could impose a strong constraint on the exponential model. Additionally, this behavior might indicate potential instability of neutron stars within the exponential model due to rotational effects, as suggested from the characteristics of  $\bar{\omega}$ , the moment of inertia, and this relation. Although previous work showed that the exponential model could accommodate up to  $2.8 M_\odot$  with  $\alpha = 1r_g^{-2}$  and  $\beta = 0.2r_g^2$ , the  $\bar{I} - C$  relation is only consistent with  $\alpha = 0.001r_g^{-2}$ . In contrast, other models yield consistent results across varying parameters, with no significant deviations, but still reflecting the influence of  $f(Q)$  modifications on the  $\bar{I} - C$  relation. The fitting coefficients derived from the best fit are presented in Table 2. From the table, we can also see the translation of the fitting coefficients due to variations in the parameters  $\alpha_i$  and  $\beta_i$ , which result in either positive or negative shifts relative to GR. It is also clear how significant the influence of these parameters is in causing deviations for each model. For example, in the exponential model, changes in  $\beta_3$  only affect the order of the coefficient  $a_1$  at  $\mathcal{O}(10^{-3})$  with the same value of  $\alpha_3$ , while in the

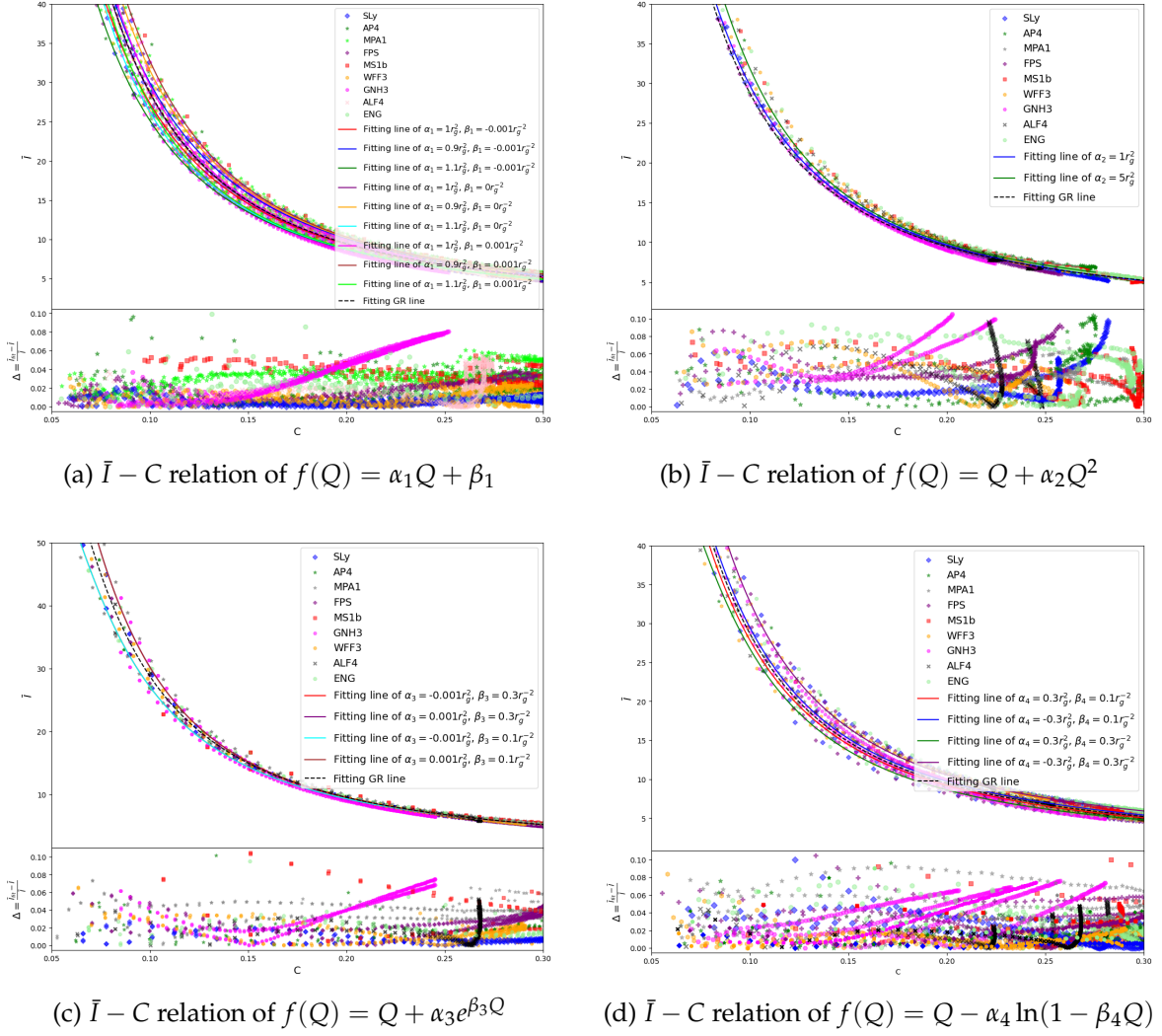
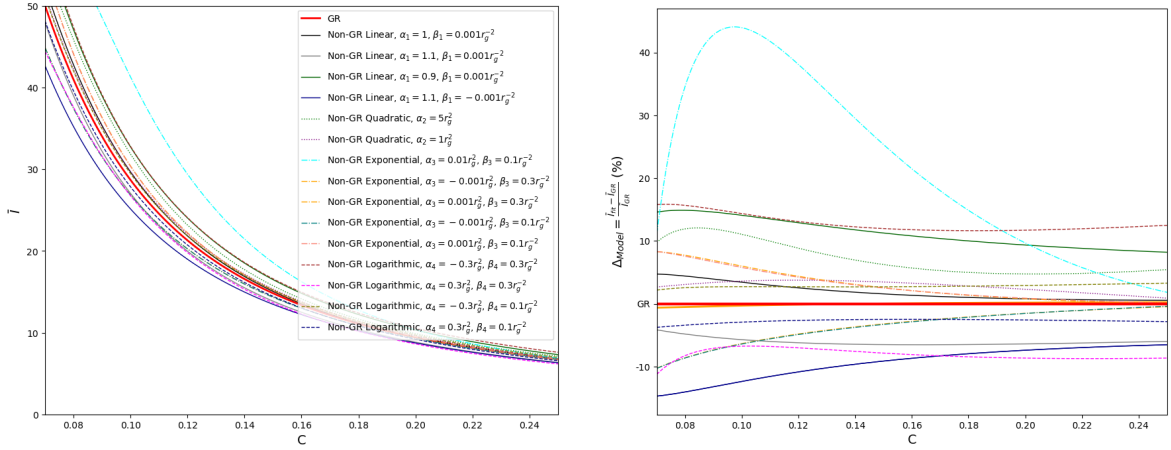


**Figure 3:** Universal  $\bar{I} - C$  relation of various  $f(Q)$  model.

logarithmic model, changes in  $\beta_4$  affect the difference in coefficients up to  $\mathcal{O}(10^{-2})$ . This is in accordance with what is depicted in Fig. 4

## 4 Conclusion

In this paper, we calculated NS properties within the framework of  $f(Q)$  gravity. First, we derived the modified TOV equations using slowly rotating metric and determined the initial values and integration limits for these equations. Then, we obtained numerical solutions using the shooting method with realistic EoS and computed the profiles of  $\bar{\omega}$  and the moment of inertia for four extended  $f(Q)$  models: linear, quadratic, logarithmic, and exponential. Based on the results, we tested their consistency with the mass-radius relation and profiles obtained in our previous work, finding that the solutions align well with the angular velocity  $\bar{\omega}$  and the corresponding moment of inertia. Finally, we calculated the universal relation



(a) The best-fitting  $\bar{I} - C$  relation from Table 2.

(b) The percentage deviation from the GR.

**Figure 4:** The best-fitting  $\bar{I} - C$  relation for GR and all  $f(Q)$  models with various parameters  $\alpha$  and  $\beta$ . The percentage deviation of the best-fitting  $\bar{I} - C$  relation for each model from the GR best-fitting relation in this calculation is also shown. The orange solid line represents the difference between our GR calculation and the results from [57], which is approximately 4%.

between the moment of inertia and the compactness of the star.

Non-metricity, as the main geometric component in this study, influences the distribution of the geometric profiles  $A(r)$  and  $B(r)$ , leading to deviations in the properties of the star. This also affects the angular velocity and the moment of inertia of NS in the slowly rotating case. In  $f(Q)$  models, deviations in the angular velocity are observed at the center of the star, with larger deviations corresponding to higher values of the  $f(Q)$  parameter. A similar trend is observed in the moment of inertia, where the deviations are even more pronounced than those in the maximum mass. This makes the moment of inertia a potentially good constraint for gravitational theories, offering the possibility to probe or even rule them out. We further explored the universal  $\bar{I} - C$  relation, finding that using  $I/M^3$  as a function of compactness demonstrates good universality within the  $f(Q)$  theory, consistent with [57], with residuals around 10%. In the slowly rotating case, the rotational effects in each model exhibit consistent behavior with the obtained values of  $I$  and correlate well with the mass-radius relation. However, the exponential model is notable, as its rotational effects are relatively more pronounced, showing some deviations when  $\alpha$  exceeds 0.01. This presents a limitation for the exponential model, especially if the observed  $\bar{I} - C$  relation shows minimal deviation from GR. In contrast, models that show relatively large deviations in maximum mass, such as the logarithmic model, demonstrate more stable and consistent deviations as the parameters change, as illustrated in Fig. 4b.

In this paper, we also tested the hybrid star EoS (ALF4) and quark star EoS (SQM). The results obtained are consistent with the behavior observed in the calculation of the  $\bar{I} - C$  relation for PSR J0737-3039A, where the moment of inertia of a quark star is larger than that of



a hybrid star, in agreement with references in alternative gravity theories such as  $f(R)$ . This result is also similar with calculations in binary systems containing pulsars, such as the moment of inertia calculation for the PSR J0737-3039A system [74]. By using gravitational wave data from LIGO/Virgo (GW170817 and GW190425), which constrain tidal deformability ( $\Lambda$ ), and mass-radius measurements from NICER (PSR J0030+0415 and PSR J0740+6620), it is possible to estimate the moment of inertia of PSR J0737-3039A. Bayesian analysis suggests that the moment of inertia of this pulsar is approximately  $\sim 1.30 \times 10^{45} \text{ g cm}^2$ , depending on the employed hadronic EoS. Furthermore, these measurements allow the study of possible phase transitions in the core of pulsars, such as transitions from hadronic to quark matter. If PSR J0737-3039A is a quark star, its moment of inertia is expected to be larger, around  $\sim 1.55 \times 10^{45} \text{ g cm}^2$ . This suggests that accurate measurements of  $I$  could help distinguish between hadronic neutron stars, hybrid stars, and quark stars. In this paper, we did not focus extensively on quark star EoS, making it an interesting topic for future work.

With more accurate measurements of the moment of inertia in the future, this universal  $\bar{I} - C$  relation can be used to test the consistency of observational data with GR or alternative gravity theories, while simultaneously constraining high-density matter EoS models. For example, the best-fit results from Fig. 4a can be used to constrain the  $\alpha_i$  and  $\beta_i$  parameters of the  $f(Q)$  gravity model using the  $\bar{I} - C$  relation constraint from observational data, making  $f(Q)$  one of the modified gravity theories that possibly can be tested in strong-field regimes through this relation. This universal relation works well not only for the slowly rotating case but also for rapidly rotating and even extreme rotating cases, which have been studied in several other gravity models [75, 76]. It would certainly be interesting to explore this within the  $f(Q)$  model, as it is likely to yield similar conclusions. However, this approach will involve more complex calculations due to the non-metricity, which changes at  $\mathcal{O}(e^2)$  and higher orders. Additionally, it would be interesting to explore other neutron star properties in future work within the  $f(Q)$  model, such as tidal deformability, quadrupole moment, and quasinormal modes, which could provide additional universal relations like the  $I - \text{Love} - Q$  [20, 77] or  $I - \text{Love} - C$  relations [78–80], offering better accuracy than the  $\bar{I} - C$  relation.

## Acknowledgments

The authors thank R. Saito and N. Yoshioka for the useful discussion. MAA would also like to thank M. D. Danarianto for his helpful discussion regarding numerical methods on neutron stars. BM thanks IUCAA, Pune (India) for providing support in the form of an academic visit during which this work is accomplished.

## A Fitting Coefficients from the best-fit of each model

We present a table summarizing the fitting coefficients obtained for various parameter values. The GR coefficients derived in this study have been compared with those reported by [57], revealing a difference of approximately 4% from our fitting results, which is consistent with other studies using modified gravity, such as [22]. Notably, the fitting coefficients in

linear  $f(Q)$  gravity reduce to their GR counterparts when  $\alpha_1 = 1$  and  $\beta_1 = 0$ , with only a minor deviation of about 0.6% at low compactness, which further decreases to approximately 0.2% at high compactness.

**Table 2:** Fitting coefficients for various  $f(Q)$  models.

Model Parameters			Fitting Coefficients			
$f(Q)$ Model	$\alpha_i$	$\beta_i$	$a_1$	$a_2$	$a_3$	$a_4$
<b>GR</b>	-	-	0.984850	0.148325	0.008787	-0.000478
$\alpha_1 Q + \beta_1$	0.9	$-0.001 r_g^{-2}$	0.940044	0.209700	0.003478	-0.000390
		$0 r_g^{-2}$	1.022874	0.163298	0.011448	-0.000647
		$0.001 r_g^{-2}$	1.065034	0.137465	0.016508	-0.000818
	1.0	$-0.001 r_g^{-2}$	0.927191	0.183875	0.000258	-0.000289
		$0 r_g^{-2}$	0.981338	0.152732	0.008080	-0.000457
		$0.001 r_g^{-2}$	1.050027	0.115086	0.014389	-0.000673
	1.1	$-0.001 r_g^{-2}$	0.891082	0.170076	0.001210	-0.000199
		$0 r_g^{-2}$	0.965761	0.131052	0.007282	-0.000382
		$0.001 r_g^{-2}$	1.006123	0.108109	0.011356	-0.000518
$Q + \alpha_2 Q^2$	$r_g^2$	-	0.807455	0.214525	0.003795	-0.000360
	$5r_g^2$	-	1.481620	-0.055989	0.039296	-0.001666
$Q + \alpha_3 e^{\beta_3 Q}$	$-0.001 r_g^2$	$0.1 r_g^{-2}$	1.033401	0.142037	0.006790	-0.000448
		$0.3 r_g^{-2}$	1.016231	0.148039	0.006198	-0.000430
	$0.001 r_g^2$	$0.1 r_g^{-2}$	1.032616	0.111374	0.016211	-0.000733
		$0.3 r_g^{-2}$	1.041438	0.104906	0.017337	-0.000784
$Q - \alpha_4 \ln(1 - \beta_4 Q)$	$-0.3 r_g^2$	$0.1 r_g^{-2}$	1.085942	0.125431	0.012198	-0.000613
		$0.3 r_g^{-2}$	1.350066	0.060585	0.023104	-0.000986
	$0.3 r_g^2$	$0.1 r_g^{-2}$	0.905931	0.163995	0.006560	-0.000417
		$0.3 r_g^{-2}$	1.065275	0.048083	0.022113	-0.001083

## References

- [1] T. Baker, D. Psaltis and C. Skordis, *Linking Tests of Gravity On All Scales: from the Strong-Field Regime to Cosmology*, *Astrophys. J.* **802** (2015) 63 [[1412.3455](#)].
- [2] C. Bambi and A. Cardenas-Avendano, eds., *Recent Progress on Gravity Tests. Challenges and Future Perspectives*, Springer Series in Astrophysics and Cosmology, Springer (2024), [10.1007/978-981-97-2871-8](#).
- [3] LIGO SCIENTIFIC, VIRGO collaboration, *Tests of general relativity with GW150914*, *Phys. Rev. Lett.* **116** (2016) 221101 [[1602.03841](#)].
- [4] LIGO SCIENTIFIC, VIRGO collaboration, *Tests of General Relativity with GW170817*, *Phys. Rev. Lett.* **123** (2019) 011102 [[1811.00364](#)].
- [5] LIGO SCIENTIFIC, VIRGO collaboration, *Tests of general relativity with binary black holes from the second LIGO-Virgo gravitational-wave transient catalog*, *Phys. Rev. D* **103** (2021) 122002 [[2010.14529](#)].
- [6] LIGO SCIENTIFIC, VIRGO collaboration, *GW150914: First results from the search for binary black hole coalescence with Advanced LIGO*, *Phys. Rev. D* **93** (2016) 122003 [[1602.03839](#)].
- [7] L. Shao and K. Yagi, *Neutron stars as extreme laboratories for gravity tests*, *Sci. Bull.* **67** (2022) 1946 [[2209.03351](#)].
- [8] M. Linares, T. Shahbaz and J. Casares, *Peering into the dark side: Magnesium lines establish a massive neutron star in PSR J2215+5135*, *Astrophys. J.* **859** (2018) 54 [[1805.08799](#)].
- [9] M. Burgay et al., *An Increased estimate of the merger rate of double neutron stars from observations of a highly relativistic system*, *Nature* **426** (2003) 531 [[astro-ph/0312071](#)].
- [10] A.G. Lyne et al., *A Double - pulsar system - A Rare laboratory for relativistic gravity and plasma physics*, *Science* **303** (2004) 1153 [[astro-ph/0401086](#)].
- [11] J.M. Lattimer and B.F. Schutz, *Constraining the equation of state with moment of inertia measurements*, *Astrophys. J.* **629** (2005) 979 [[astro-ph/0411470](#)].
- [12] P. Landry and B. Kumar, *Constraints on the moment of inertia of PSR J0737-3039A from GW170817*, *Astrophys. J. Lett.* **868** (2018) L22 [[1807.04727](#)].
- [13] S.S. Yazadjiev, D.D. Doneva, K.D. Kokkotas and K.V. Staykov, *Non-perturbative and self-consistent models of neutron stars in R-squared gravity*, *JCAP* **06** (2014) 003 [[1402.4469](#)].
- [14] S. Capozziello, M. De Laurentis, R. Farinelli and S.D. Odintsov, *Mass-radius relation for neutron stars in  $f(R)$  gravity*, *Phys. Rev. D* **93** (2016) 023501 [[1509.04163](#)].
- [15] E. Babichev, K. Koyama, D. Langlois, R. Saito and J. Sakstein, *Relativistic Stars in Beyond Horndeski Theories*, *Class. Quant. Grav.* **33** (2016) 235014 [[1606.06627](#)].
- [16] A.V. Astashenok, S. Capozziello, S.D. Odintsov and V.K. Oikonomou, *Causal limit of neutron star maximum mass in  $f(R)$  gravity in view of GW190814*, *Phys. Lett. B* **816** (2021) 136222 [[2103.04144](#)].
- [17] R.-H. Lin, X.-N. Chen and X.-H. Zhai, *Realistic neutron star models in  $f(T)$  gravity*, *Eur. Phys. J. C* **82** (2022) 308 [[2109.00191](#)].
- [18] Z. Liu, Z. Li, L. Liang, S. Li and H. Yu, *Neutron stars in Gauss-Bonnet extended Starobinsky gravity*, *Phys. Rev. D* **110** (2024) 124052 [[2410.14108](#)].

- [19] Y.-X. Cui, Z. Yan, K. Numajiri, T. Katsuragawa and S. Nojiri, *Compact star in a noninteger power model of  $f(R)$  gravity*, *Phys. Rev. D* **110** (2024) 084028 [2408.12301].
- [20] K. Yagi and N. Yunes, *I-Love-Q*, *Science* **341** (2013) 365 [1302.4499].
- [21] K.V. Staykov, D.D. Doneva and S.S. Yazadjiev, *Moment-of-inertia–compactness universal relations in scalar-tensor theories and  $\mathcal{R}^2$  gravity*, *Phys. Rev. D* **93** (2016) 084010 [1602.00504].
- [22] J. Sakstein, E. Babichev, K. Koyama, D. Langlois and R. Saito, *Towards strong field tests of beyond Horndeski gravity theories*, *Phys. Rev. D* **95** (2017) 064013.
- [23] H. Boumaza, *Slowly rotating neutron stars in scalar torsion theory*, *Eur. Phys. J. C* **81** (2021) 448.
- [24] J.L. Blázquez-Salcedo, L.M. González-Romero, F.S. Khoo, J. Kunz and V. Preut, *Universal relations for quasinormal modes of neutron stars in  $R^2$  gravity*, *Phys. Rev. D* **106** (2022) 044007 [2205.03283].
- [25] R. Xu, Y. Gao and L. Shao, *Neutron stars in massive scalar-Gauss-Bonnet gravity: Spherical structure and time-independent perturbations*, *Phys. Rev. D* **105** (2022) 024003 [2111.06561].
- [26] M. Murshid and M. Kalam, *Neutron stars in  $f(R,T)$  theory: slow rotation approximation*, *JCAP* **09** (2024) 030 [2306.13758].
- [27] E.J. Copeland, M. Sami and S. Tsujikawa, *Dynamics of Dark Energy*, *Int. J. Mod. Phys. D* **15** (2006) 1753.
- [28] T. Clifton and P. G. Ferreira and A. Padilla and C. Skordis, *Modified gravity and cosmology*, *Phys. Rep.* **513** (2012) 1.
- [29] A. Joyce, B. Jain, J. Khoury and M. Trodden, *Beyond the cosmological standard model*, *Physics Reports* **568** (2015) 1.
- [30] K. Koyama, *Cosmological tests of modified gravity*, *Rep. Prog. Phys.* **79** (2016) 046902.
- [31] P. Bull, Y. Akrami, J. Adamek, T. Baker et al., *Beyond  $\Lambda$ CDM: Problems, solutions, and the road ahead*, *Physics of the Dark Universe* **12** (2016) 56.
- [32] J.B. Jiménez, L. Heisenberg and T. Koivisto, *Coincident general relativity*, *Phys. Rev. D* **98** (2018) 044048.
- [33] T. Harko, T.S. Koivisto, F.S.N. Lobo, G.J. Olmo and D. Rubiera-Garcia, *Coupling matter in modified  $Q$  gravity*, *Phys. Rev. D* **98** (2018) 084043.
- [34] F.K. Anagnostopoulos, S. Basilakos and E.N. Saridakis, *First evidence that non-metricity  $f(Q)$  gravity could challenge  $\Lambda$ CDM*, *Phys. Lett. B* **822** (2021) 136634.
- [35] F.K. Anagnostopoulos, V. Gakis, E.N. Saridakis and S. Basilakos, *New models and big bang nucleosynthesis constraints in  $f(Q)$  gravity*, *Eur. Phys. J. C* **83** (2023) 58.
- [36] L. Heisenberg, M. Hohmann and S. Kuhn, *Homogeneous and isotropic cosmology in general teleparallel gravity*, *Eur. Phys. J. C* **83** (2023) 315.
- [37] S. Nojiri and S.D. Odintsov, *Well-defined  $f(Q)$  gravity, reconstruction of FLRW spacetime and unification of inflation with dark energy epoch*, *Phys. Dark Univ.* **45** (2024) 101538 [2404.18427].
- [38] W. Khyllep, A. Paliathanasis and J. Dutta, *Cosmological solutions and growth index of matter perturbations in  $f(Q)$  gravity*, *Phys. Rev. D* **103** (2021) 103521.
- [39] M. Koussour, S. Shekh and M. Bennai, *Anisotropic nature of space-time in  $f(Q)$  gravity*, *Phys. Dark Universe* **36** (2022) 101051.

- [40] N. Frusciante, *Signatures of  $f(Q)$  gravity in cosmology*, *Phys. Rev. D* **103** (2021) 044021.
- [41] S. Narawade, L. Pati, B. Mishra and S. Tripathy, *Dynamical system analysis for accelerating models in non-metricity  $f(Q)$  gravity*, *Phys. Dark Universe* **36** (2022) 101020.
- [42] S.A. Narawade and B. Mishra, *Phantom Cosmological Model with Observational Constraints in  $f(Q)$  Gravity*, *Ann. Phys.* **535** (2023) 2200626.
- [43] L. Heisenberg and M. Hohmann, *Gauge-invariant cosmological perturbations in general teleparallel gravity*, *Eur. Phys. J. C* **84** (2024) 462 [2311.05597].
- [44] F. D'Ambrosio, S.D.B. Fell, L. Heisenberg and S. Kuhn, *Black holes in  $f(Q)$  gravity*, *Phys. Rev. D* **105** (2022) 024042 [2109.03174].
- [45] S.K. Maurya, K.N. Singh, S.V. Lohakare and B. Mishra, *Anisotropic Strange Star Model Beyond Standard Maximum Mass Limit by Gravitational Decoupling in  $f(Q)$  Gravity*, *Fortschritte der Phys.* **70** (2022) 2200061.
- [46] M.A. Alwan, T. Inagaki, B. Mishra and S. Narawade, *Neutron star in covariant  $f(Q)$  gravity*, *J. Cosmol. Astropart. Phys.* **2024** (2024) 011.
- [47] P. Bhar and J.M.Z. Pretel, *Dark energy stars and quark stars within the context of  $f(Q)$  gravity*, *Phys. Dark Universe* **42** (2023) 101322.
- [48] P. Bhar, K.N. Singh, S.K. Maurya and M. Govender, *A four parameters quark star in quadratic  $f(Q)$ -action*, *Phys. Dark Universe* **43** (2024) 101391.
- [49] S.V. Lohakare, S.K. Maurya, K.N. Singh, B. Mishra and A. Errehymy, *Influence of three parameters on maximum mass and stability of strange star under linear  $f(Q)$  – action*, *Mon. Notices Royal Astron. Soc.* **526** (2023) 3796.
- [50] M.Z. Gul, S. Rani, M. Adeel and A. Jawad, *Viable and stable compact stars in  $f(Q)$  theory*, *Eur. Phys. J. C* **84** (2024) 8.
- [51] J.B. Jiménez, L. Heisenberg, T. Koivisto and S. Pekar, *Cosmology in  $f(Q)$  geometry*, *Phys. Rev. D* **101** (2020) 103507.
- [52] D. Zhao, *Covariant formulation of  $f(Q)$  theory*, *Eur. Phys. J. C* **82** (2022) 303.
- [53] R.-H. Lin and X.-H. Zhai, *Spherically symmetric configuration in  $f(Q)$  gravity*, *Phys. Rev. D* **103** (2021) 124001.
- [54] J.-T. Beh, T.-H. Loo and A. De, *Geodesic deviation equation in  $f(Q)$ -gravity*, *Chin. J. Phys.* **77** (2022) 1551.
- [55] G. Subramaniam, A. De, T.-H. Loo and Y.K. Goh, *How different connections in flat FLRW geometry impact energy conditions in  $f(Q)$  theory?*, *Fortschritte der Phys.* **71** (2023) 2300038.
- [56] J.B. Hartle, *Slowly Rotating Relativistic Stars. I. Equations of Structure*, *Astrophys. J.* **150** (1967) 1005.
- [57] C. Breu and L. Rezzolla, *Maximum mass, moment of inertia and compactness of relativistic stars*, *Mon. Not. Roy. Astron. Soc.* **459** (2016) 646.
- [58] S. Chaudharya, S.K. Maurya, J. Kumara and G. Mustafa, *Most general isotropic charged fluid solution for Buchdahl model in  $\mathcal{F}(Q)$  gravity*, *J. Cosmol. Astropart. Phys.* **09** (2024) 049.
- [59] F. Douchin and P. Haensel, *A unified equation of state of dense matter and neutron star structure*, *Astron. Astrophys.* **380** (2001) 151.

- [60] Kalin V. Staykov and Daniela D. Doneva and Stoytcho S. Yazadjiev and Kostas D. Kokkotas, *Slowly rotating neutron and strange stars in  $R^2$  gravity*, *Journal of Cosmology and Astroparticle Physics* **2014** (2014) 006.
- [61] J. Näf and P. Jetzer, *On the  $1/c$  expansion of  $f(R)$  gravity*, *Phys. Rev. D* **81** (2010) 104003.
- [62] D.G. Ravenhall and C.J. Pethick, *Neutron Star Moments of Inertia*, *Astrophys. J.* **424** (1994) 846.
- [63] A. Akmal, V.R. Pandharipande and D.G. Ravenhall, *Equation of state of nucleon matter and neutron star structure*, *Phys. Rev. C* **58** (1998) 1804.
- [64] B. Friedman and V.R. Pandharipande, *Hot and cold, nuclear and neutron matter*, *Nucl. Phys. A* **361** (1981) 502.
- [65] R.B. Wiringa, V. Fiks and A. Fabrocini, *Equation of state for dense nucleon matter*, *Phys. Rev. C* **38** (1988) 1010.
- [66] H. Mueller and B.D. Serot, *Relativistic mean field theory and the high density nuclear equation of state*, *Nucl. Phys. A* **606** (1996) 508.
- [67] L. Engvik, M. Hjorth-Jensen, E. Osnes, G. Bao and E. Ostgaard, *Asymmetric nuclear matter and neutron star properties*, *Phys. Rev. Lett.* **73** (1994) 2650.
- [68] H. MÅ¼ther, M. Prakash and T. Ainsworth, *The nuclear symmetry energy in relativistic Brueckner-Hartree-Fock calculations*, *Phys. Lett. B* **199** (1987) 469.
- [69] M. Alford, M. Braby, M.W. Paris and S. Reddy, *Hybrid stars that masquerade as neutron stars*, *Astrophys. J.* **629** (2005) 969.
- [70] N.K. Glendenning, *Neutron stars are giant hypernuclei ?*, *Astrophys. J.* **293** (1985) 470.
- [71] R.F. Sawyer, *Condensed pi- phase in neutron star matter*, *Phys. Rev. Lett.* **29** (1972) 382.
- [72] V. Canuto, *Equation of State at Ultrahigh Densities. 1.*, *Ann. Rev. Astron. Astrophys.* **12** (1974) 167.
- [73] H.C. Das, *I-Love-C relation for an anisotropic neutron star*, *Phys. Rev. D* **106** (2022) 103518 [2208.12566].
- [74] Z. Miao, A. Li and Z.-G. Dai, *On the moment of inertia of PSR J0737-3039 A from LIGO/Virgo and NICER*, *Mon. Not. Roy. Astron. Soc.* **515** (2022) 5071.
- [75] A.V. Astashenok and S.D. Odintsov, *Rotating Neutron Stars in  $F(R)$  Gravity with Axions*, *Mon. Not. Roy. Astron. Soc.* **498** (2020) 3616 [2008.11271].
- [76] D.D. Doneva and S.S. Yazadjiev, *Rapidly rotating neutron stars with a massive scalar field—structure and universal relations*, *JCAP* **11** (2016) 019 [1607.03299].
- [77] K. Yagi and N. Yunes, *I-Love-Q Relations in Neutron Stars and their Applications to Astrophysics, Gravitational Waves and Fundamental Physics*, *Phys. Rev. D* **88** (2013) 023009 [1303.1528].
- [78] A. Maselli, V. Cardoso, V. Ferrari, L. Gualtieri and P. Pani, *Equation-of-state-independent relations in neutron stars*, *Phys. Rev. D* **88** (2013) 023007 [1304.2052].
- [79] K. Yagi and N. Yunes, *Approximate Universal Relations for Neutron Stars and Quark Stars*, *Phys. Rept.* **681** (2017) 1 [1608.02582].
- [80] N. Jiang and K. Yagi, *Analytic I-Love-C relations for realistic neutron stars*, *Phys. Rev. D* **101** (2020) 124006 [2003.10498].